

AMPLITUDE-PHASE ANALYSIS OF COSMIC MICROWAVE BACKGROUND MAPS

P. Naselsky², D.Novikov^{1,3} and Joseph Silk¹.

¹ Astronomy Department, University of Oxford, NAPL, Keble Road,
Oxford OX1 3RH, UK

² Theoretical Astrophysics Center, Juliane Maries Vej 30, DK-2100
Copenhagen, Denmark

³ Astro-Space Center of P.N.Lebedev Physical Institute, Profsouznaya 84/32,
Moscow, Russia,

⁴ Rostov State University, Zorge 5, Rostov-on-Don, Russia

Abstract

We propose a novel method for the extraction of unresolved point sources from CMB maps. This method is based on the analysis of the phase distribution of the Fourier components for the observed signal and unlike most other methods of denoising does not require any significant assumptions about the expected CMB signal. The aim of our paper is to show how, using our algorithm, the contribution from point sources can be separated from the resulting signal on all scales. We believe that this technique is potentially a very powerful tool for extracting this type of noise from future high resolution maps.

Subject headings: cosmic microwave background, cosmology, statistics, observations.

1 Introduction

Observations of the Cosmic Microwave Background (CMB) is fundamental for our understanding the primordial inhomogeneity of the Universe. After the successful COBE experiment, attention has been focused on the investigation of small scale perturbations, that can provide unique information about the most important cosmological parameters. One of the major problems in the modern CMB cosmology is to separate noise of various origins (such as dust emission, synchrotron radiation and unresolved point sources (see e.g. Banday et al. 1996)) from the original cosmological signal. Many authors have already applied various methods such as Wiener filtering (Tegmark and Efstathiou 1996, Bouchet and Gispert 1999), maximum entropy technique (Hobson et al. 1999), radical compression (Bond et al. 1998), power filtering (Gorski et. al. 1997, Naselsky et. al. 1999) and wavelet techniques (e.g. Sanz et al. 1999) to extract noise from the CMB data.

All of these techniques have been tested for removing the noise from the real observational data. It is necessary to note that, for different strategies and for different experiments, different schemes could be chosen as most appropriate. The choice of the algorithm also depends on the particular type of foreground emission to be extracted.

The aim of our paper is to overcome the problem of detecting and extracting the background of unresolved point sources from the original map. The measured signal in the real observational data is always smoothed with some filtering angle θ_f because of the final antenna beam resolution. Therefore, unresolved point sources could make a significant contribution to the resulting signal on all scales. This type of noise should be removed from the original map before any subsequent analysis is made.

Recently (Cayon et al. 1999) have proposed the use of isotropic wavelets for removing noise in the form of point sources. Their technique is based on the fact, that the field in the vicinity of the source should be in the form of the antenna profile. Unfortunately the Gaussian CMB field can also form real peaks with the same profile, so that a lot of 'artificial sources' could be found using this technique. Besides, the antenna profile is not necessarily isotropic (indeed, as a rule it is very anisotropic). Therefore, isotropic wavelets should not be considered as an absolute cure against such a type of noise.

In this paper we consider an approach, which is based on the distribution of phases. The idea of using phases of random fields was introduced by A.Melott et al (1991); Coles and Chiang (2000a,b) for the Large Scale Structure formation in the Universe. Below we develop the phase-amplitude analysis method for investigation of the CMB anisotropy and foreground. The outline of the paper is as follows. In section 2 we briefly review the basic definitions, consider a simulated one-dimensional scan of the CMB first with a single point source, then with a background of such a sources. In section 3 we generalize our results into two-dimensional maps. Finally, we suggest an algorithm for denoising. In section 4 we discuss the results and potential of the method for analyzing high resolution maps.

2 Point sources in one-dimensional scans.

In this section we consider 1D CMB scans with a background of point sources. This approach could be very useful for data analysis of one-dimensional experiments with high resolution (such as RATAN 600). We extend this discussion to two-dimensional experiments (such as the new generation of interferometer experiments) in section 3. The investigation of point sources is especially easy in one dimension, can be easily generalized into two-dimensional maps and will help us to understand the advantage of the proposed technique.

Definitions

In 1D the deviation of the temperature from its mean value $\Delta T = T - \langle T \rangle$ in a scan is described by the simple Fourier series:

$$\Delta T(\theta) = \sum_k a_k \cos(k\theta) + b_k \sin(k\theta) \quad (1)$$

where k is an integer number and θ can be expressed in terms of the real angle on the sky (θ_{sky}) as follows: $\theta = \frac{\theta_{tot}}{2\pi} \theta_{sky}$. Here θ_{tot} means the total length of the scan.

The detected temperature fluctuations ΔT can as usual be naturally divided into two parts: cosmological signal and noise:

$$\Delta T(\theta) = \Delta T^s(\theta) + \Delta T^n(\theta) \quad (2)$$

where s and n denote signal and noise respectively. Therefore, the Fourier transform components a_k, b_k can be also expressed as a sum of Fourier decomposition of these two terms:

$$\begin{aligned} a_k &= a_k^s + a_k^n, \\ b_k &= b_k^s + b_k^n. \end{aligned} \quad (3)$$

The statistically isotropic distribution of the CMB temperature anisotropy is supposed to be in the form of a random Gaussian field with the power spectrum $P_{CMB}(k)$, which is determined by the appropriate cosmological model. The coefficients a_k^s, b_k^s depend on the spectrum of the CMB, the antenna filtering function $\tilde{F}(\theta - \theta^*, \theta_f)$ and the actual realization of the random Gaussian process on the sky. In general, they obey the formulae: $\langle a_k^s a_{k'}^s \rangle = \langle b_k^s b_{k'}^s \rangle = \delta_{kk'} F(k, k_f) P_{CMB}(k)$. Here, $F(k, k_f)$ is the Fourier transform of the filtering function and θ_f is the antenna resolution angle. k_f is a wavenumber which corresponds to this resolution: $k_f = 1/\theta_f$. In our simulations we use the usual expression for a_k, b_k :

$$\begin{aligned} a_k^s &= \alpha_k F^{\frac{1}{2}}(k, k_f) P_{CMB}^{\frac{1}{2}}(k), \\ b_k^s &= \beta_k F^{\frac{1}{2}}(k, k_f) P_{CMB}^{\frac{1}{2}}(k), \end{aligned} \quad (4)$$

where α_k, β_k are independent Gaussian numbers with zero mean and unit dispersion.

In this paper we consider the noise in the form of isolated unresolved point sources. This means that the average distance between sources is larger than the resolution scale θ_f . Therefore, the shape of the 'noise' field around the point source determined by the filtering function F :

$$\begin{aligned} \Delta T_n(\theta) &= \int \sum_{j=1}^{N_{ps}} \gamma_j \delta(\theta^* - \theta) \tilde{F}^{\frac{1}{2}}(\theta^* - \theta, \theta_f) d\theta^* = \\ &= \sum_{j=1}^{N_{ps}} \gamma_j \tilde{F}^{\frac{1}{2}}(\theta - \theta_j, \theta_f) \end{aligned} \quad (5)$$

where γ_j, θ_j are the amplitude and the position of the j -th point source, respectively, and N_{ps} is the total number of point sources in the considered scan. According to equation [5], the Fourier components of the noise can be described by the following very simple and convenient formulae:

$$\begin{aligned} a_k^n &= \sum_{j=1}^{N_{ps}} \gamma_j \cos(k\theta_j) F^{\frac{1}{2}}(k, k_f), \\ b_k^n &= \sum_{j=1}^{N_{ps}} \gamma_j \sin(k\theta_j) F^{\frac{1}{2}}(k, k_f). \end{aligned} \quad (6)$$

For further investigation we have to introduce the phase: φ_k of the k -th harmonic. Using equations [1,3] one can write:

$$\varphi_k = \arctan \left[\frac{b_k}{a_k} \right] = \arctan \left[\frac{b_k^s + b_k^n}{a_k^s + a_k^n} \right] \quad (7)$$

If the resulting field at the scales k is dominated by the Gaussian CMB signal ($S_k/N_k \gg 1$), then $\varphi_k \approx \arctg(b_k^s/a_k^s)$. In this case the phases of the k -th harmonics are random independent uncorrelated values, uniformly distributed from 0 to 2π . On the other hand, if the signal at these scales is much smaller than the noise, then the distribution of phases is determined by the positions and amplitudes of point sources on the scan. In Fig.1, we present the spectrum of CMB in one dimension $P_{CMB}(k)$ for the standard CDM model together with the spectrum of point sources. Both spectra are smoothed with the Gaussian filtering function $F(k, k_f) = \exp(-\frac{k^2}{2k_f^2})$. It is well known that the CMB signal disappears when k becomes larger than some value k_d . This value corresponds to the damping scale of the CMB fluctuations. Therefore, at the small scales the resulting field is dominated by the noise. Note that k_d should not be necessarily interpreted as the damping scale. Roughly speaking, this is the scale where noise from sources becomes larger than the CMB signal.

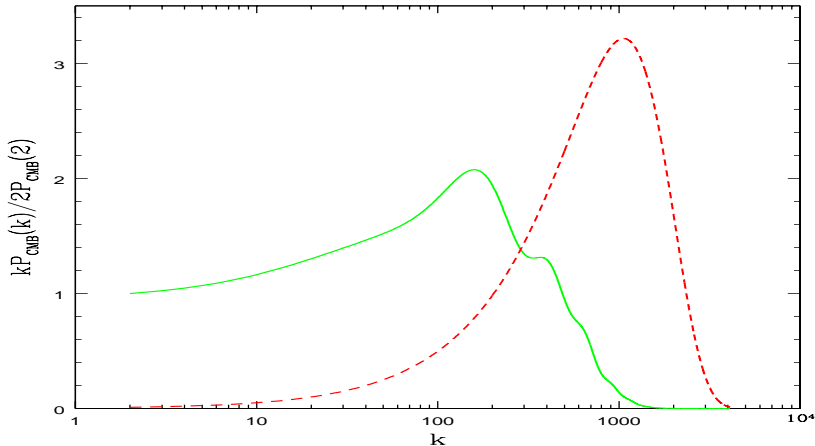


Fig. 1 The power spectrum of the CMB (solid line) for one-dimensional (360°) scan together with the spectrum of point sources (dashed line).

It is easy to see, from equations [4,6,7], that the process of smoothing does not change the phases of the primordial signal. The filtering function $F(k, k_f)$ has simply disappeared from the right hand side of the equation [7]. Therefore, if $k_f > k_d$, we have the possibility of measuring the phases only for high k values of the noise. Below we describe how the information about the phase distribution for high values of k can be used for very precise detection and extraction of the contribution from the sources for all values of k .

Detection of a single point source

Let us consider the simplest example by dealing with a single unresolved point source on the scan. In order to remove the contribution from this source, we have to know its precise

location θ_1 and amplitude γ_1 (see Fig.2).

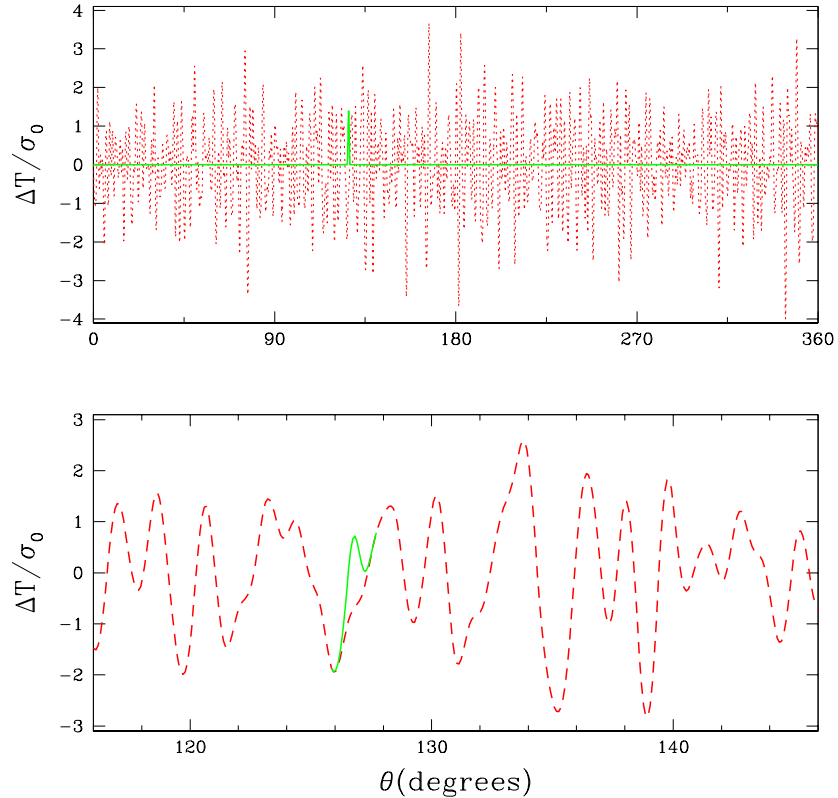


Fig. 2 Upper panel: simulated CMB field on 100° scan (1° corresponds to $\approx 0.03^\circ$ on the sky) (dashed line) and the field from a single point source (solid line). Lower panel: the same as the upper one, but with better resolution. The field in the vicinity of the point source behaves like an ordinary Gaussian fluctuation.

The contribution from this source to the resulting field according to equation [5] is then:

$$\Delta T_n = \sum_{k=1}^{k_{max}} \gamma_1 \cos(k(\theta - \theta_1)) F^{\frac{1}{2}}(k, k_f) \quad (8)$$

where k_{max} is the maximum value of k that can be detected in the experiment.

As has been already mentioned, for k larger then some value k_d , phases φ_k are just the phases of the point source. From equations [6,7], we obtain:

$$\varphi_k = \text{mod}_{2\pi}(k\theta_1) \quad (9)$$

It suffices to have only two phases (for example φ_k and φ_{k+1} , $k > k_d$) to find the location of the source θ_1 :

$$\theta_1 = \varphi_{k+1} - \varphi_k \quad (10)$$

In Fig.3 we show the behavior of the phases φ_k , $1 < k < k_{max}$ together with the phases of the source. For small values of k : $k \ll k_d$ the phases are distributed uniformly and at large k we can definitely see the regular structure that is consistent with equation [9].

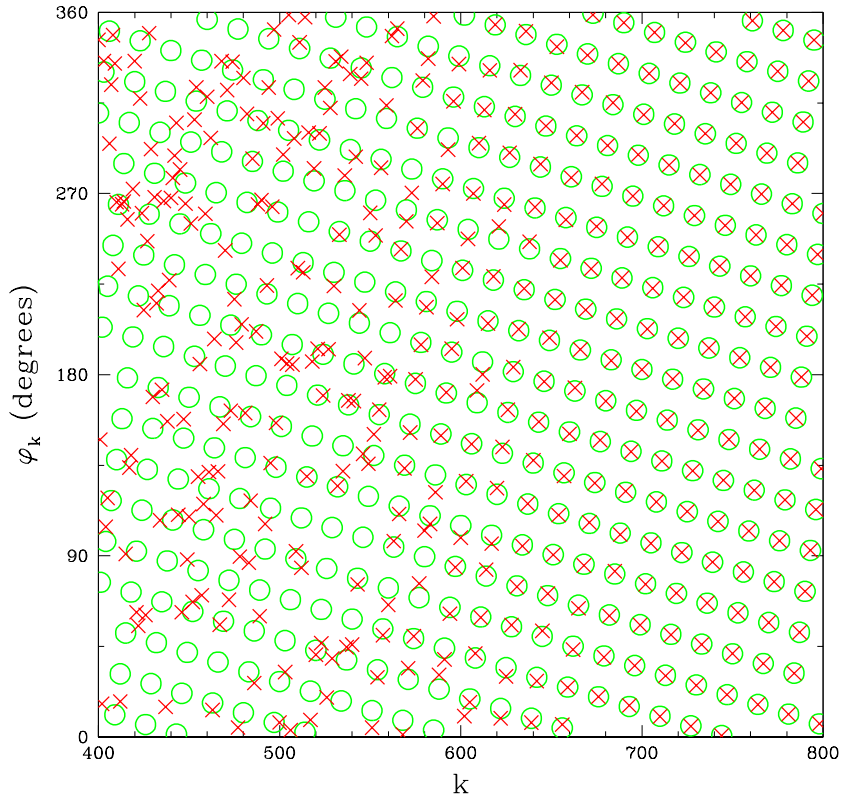


Fig. 3 The phases of the point source (circles) and phases of the resulting signal: CMB + Point source (crosses).

In Fig.4 we also show the positions of maxima for all harmonics. Location of the maxima for the k -th harmonic can be found by the formulae:

$$\theta_{max}^k = \frac{\varphi_k + 2\pi * n}{k} \quad (11)$$

where n is an integer number. The straight vertical line points to the location of the source because one of the maxima in each harmonic is coincident with this location.

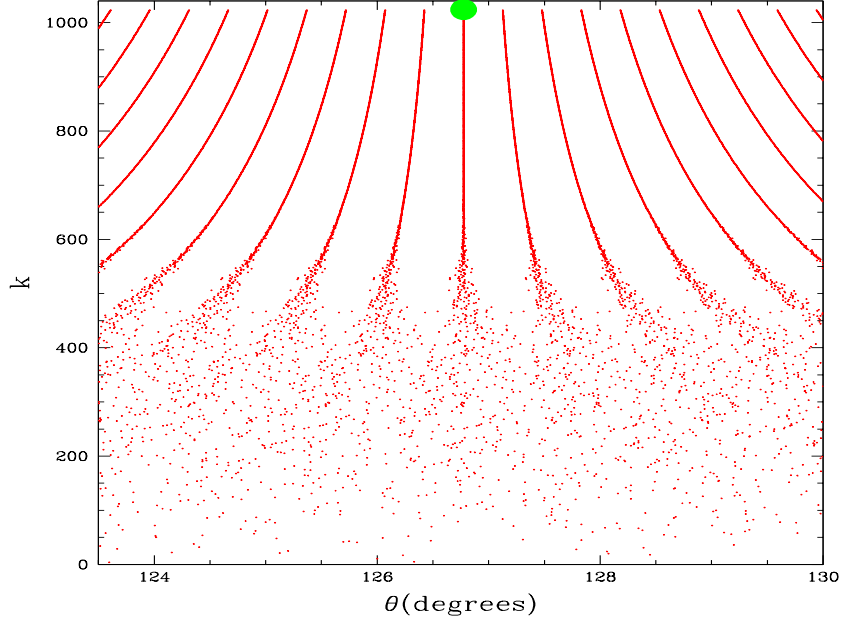


Fig. 4 Positions of maxima for each harmonic. Each point represents the positions of maxima for the k -th harmonic. For small k they are distributed uniformly (according to the Gaussian distribution of the CMB). The large dot shows the location of the source.

The remaining part of the problem is to find the amplitude - γ_1 . Let us defined the field $\Delta T^{k_d}(\theta)$ as a part of the field $\Delta T(\theta)$ that consists only of the high harmonics:

$$\Delta T^{k_d}(\theta) = \sum_{k=k_d}^{k_{max}} a_k \cos(k\theta) + b_k \sin(k\theta) \quad (12)$$

Using the formulae [8], we now can write down the obvious relation:

$$\gamma_1 = \Delta T^{k_d}(\theta_1) / \sum_{k=k_d}^{k_{max}} F(k, k_f) \quad (13)$$

Therefore, according to [3,6], we have found the contribution from this source to all harmonics from $k = 1$ to $k = k_{max}$.

Background of point sources

In this subsection we generalize our algorithm to the case where there are an unknown number of point sources in the considered scan. In a situation like this, we have to find not only positions and amplitudes of each source but also the total number of them: N_{ps} .

We believe that many different techniques based on the results of the previous subsection could be proposed to solve this problem. We suggest a simple iteration scheme. As has been already noticed above, we can consider the field ΔT^{k_d} , which consists only of high harmonics. Therefore, only point sources make a contribution to this field:

$$\begin{aligned}\Delta T^{k_d}(\theta) &= \sum_{k=k_d}^{k_{max}} a_k^n \cos(k\theta) + b_k^n \sin(k\theta) = \\ &= \sum_{j=1}^{N_{ps}} \gamma_j \sum_{k=k_d}^{k_{max}} F^{\frac{1}{2}}(k, k_f) \cos(k(\theta - \theta_j))\end{aligned}\tag{14}$$

We now introduce the filter function $L(k) = F(k - k_d, k_l)/F(k, k_f)$ and consider the filtered field:

$$\Delta \tilde{T}_k^{k_d} = \Delta T_k^{k_d} L^{\frac{1}{2}}(k)\tag{15}$$

According to [14,15], one can write:

$$\begin{aligned}\Delta \tilde{T}^{k_d}(\theta) &= \\ &= \sum_{j=1}^{N_{ps}} \gamma_j \cos(k_d(\theta - \theta_j)) \sum_{k=1}^{k_{max}-k_d} \cos(k(\theta - \theta_j)) F(k, k_l)^{\frac{1}{2}} \\ &\quad - \sin(k_d(\theta - \theta_j)) \sum_{k=1}^{k_{max}-k_d} \sin(k(\theta - \theta_j)) F(k, k_l)^{\frac{1}{2}}\end{aligned}\tag{16}$$

If we can put $k_l \ll k_d \ll k_{max}$, then the second term on the right hand side of equation [16] is small and:

$$\Delta \tilde{T}^{k_d}(\theta) \approx \sum_{j=1}^{N_{ps}} \gamma_j \sum_{k=1}^{k_{max}-k_d} \cos(k(\theta - \theta_j)) F(k, k_l)^{\frac{1}{2}}\tag{17}$$

This equation is very close to [8] and, therefore, the procedure of filtering gives us the possibility of 'localizing' the field in the vicinity of a point source.

In reality equation [17] is not quite correct because k_d and k_{max} are values of approximately the same order and, therefore, peaks, that are more or less close to each other can interfere (fig. 4). This is the reason why we choose the iteration technique to remove point sources.

We propose the following algorithm. Let us construct the field $\Delta \tilde{T}_0^{k_d} = \Delta \tilde{T}^{k_d}$ and find its highest maximum. This maximum most probably corresponds to the most powerful isolated point source on the scan. The position and value of this maximum give us the location θ_1 and the amplitude γ_1 (eq[13]) of this source. After that, we construct the field $\Delta \tilde{T}_1^{k_d}$ 'without' this point source:

$$\Delta \tilde{T}_1^{k_d}(\theta) = \Delta \tilde{T}_0^{k_d}(\theta) - \gamma_1 \sum_{k=k_d}^{k_{max}} \cos(k(\theta - \theta_1)) L(k, k_l)^{\frac{1}{2}}.\tag{18}$$

The contribution from this source to the field and its interference with other sources is now removed. This allows us to find more precisely the next highest maximum. Therefore, we apply the same procedure to the field $\Delta \tilde{T}_1^{k_d}$ and find θ_2, γ_2 and so on (Fig.5).

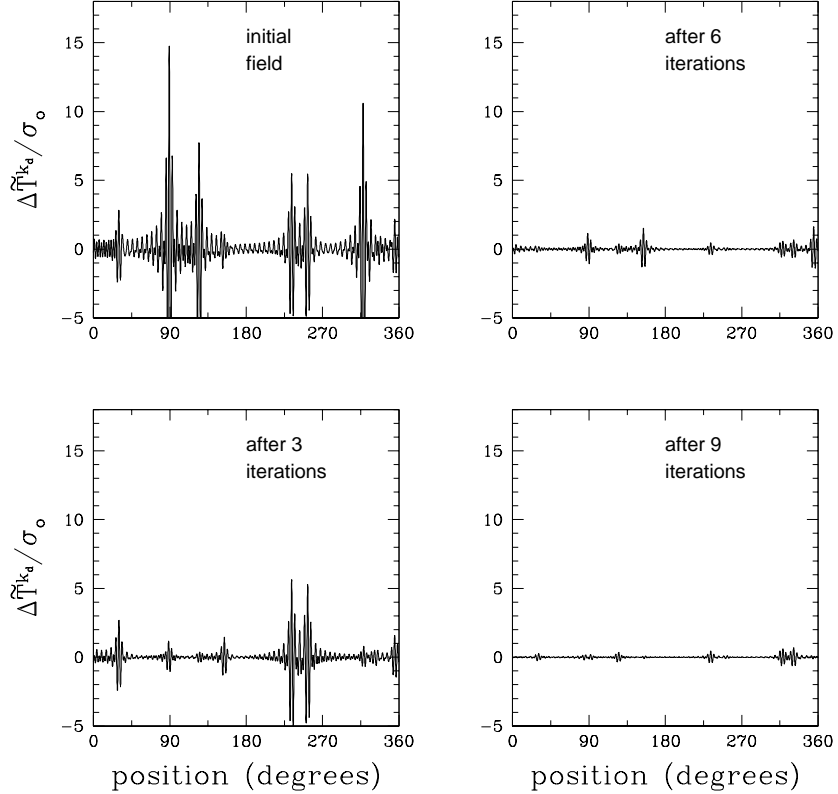


Fig. 5 The iteration scheme. Each panel represents the residuals $\Delta\tilde{T}_i^{k_d}$ from the initial field $\Delta\tilde{T}_o^{k_d} = \Delta\tilde{T}^{k_d}$ after the i -th iteration.

We perform these iterations until the dispersion $\sigma_i^{k_d}$ ($(\sigma_i^{k_d})^2 = \langle (\Delta\tilde{T}_i^{k_d})^2 \rangle$) becomes significantly smaller than $\sigma_o^{k_d}$ (Fig.6). The total number of iterations that is needed to significantly reduce the initial dispersion gives us approximately the number of point sources N_{ps} and each iteration gives the location θ_i and the amplitude γ_i of the i -th source. Note, that

$$(\sigma_i^{k_d})^2 = \sum_j \gamma_j^2, \quad \gamma_j < \gamma_i \quad (19)$$

and roughly speaking, in Fig.7 we can see the cumulative distribution of point sources over the power γ . Finally, since we have the position θ_i and amplitude γ_i , the contribution to the field from all point sources may be removed in the same manner, as was done for a single point source in the previous subsection.

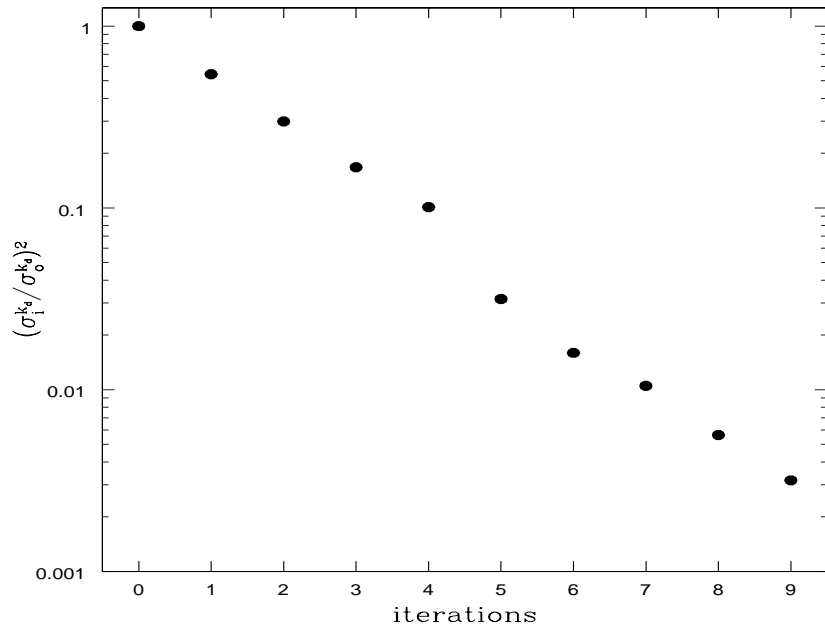


Fig. 6 The decrease of the dispersion for $\tilde{\Delta T}^{k_d}$ with each iteration.

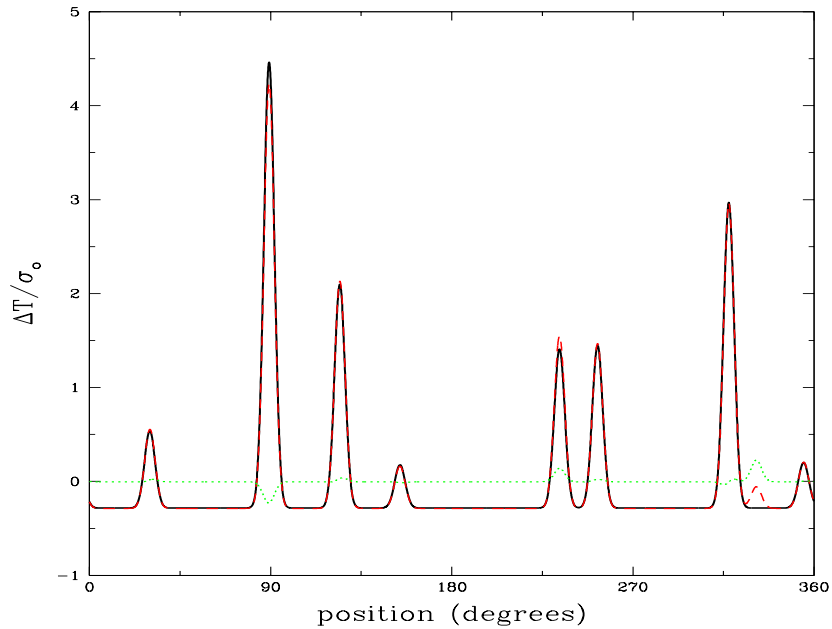


Fig. 7 The final result. The initial field of point sources (solid line), restored field by our method (dashed line), and residuals (dotted line).

3 Point sources in two dimensions.

In this section we briefly describe our results in two dimensions. Without loss of generality we may consider a small region of the sky and assume that the geometry is approximately flat. Under this assumption, the part of the detected signal which is determined by the noise associated with N_{ps} point sources can be represented according to the previous section by writing:

$$\Delta T_n(\vec{x}) = \sum_{\vec{k}} a_{\vec{k}}^n \cos(\vec{k}\vec{x}) + b_{\vec{k}}^n \sin(\vec{k}\vec{x}) = \sum_{j=1}^{N_{ps}} \gamma_j \sum_{\vec{k}} F^{\frac{1}{2}}(\vec{k}, |\vec{k}_f|) \cos(\vec{k}(\vec{x} - \vec{x}_j)) \quad (20)$$

where \vec{x}_j is the position of the j -th point source in the Cartesian coordinate system and $|\vec{k}_f|$ corresponds to the antenna resolution. Analogously to the one-dimensional case, this field should be filtered with some appropriate function. The convenient filter function $L(\vec{k})$ that we use in this case is as follows:

$$\begin{aligned} L(\vec{k}) &= F^{-1}(\vec{k}, |\vec{k}_f|) & \text{if } |\vec{k}_d| < |\vec{k}| < |\vec{k}_{max}|, \\ L(\vec{k}) &= 0 & \text{if } |\vec{k}| < |\vec{k}_d| \text{ or } |\vec{k}| > |\vec{k}_{max}|. \end{aligned} \quad (21)$$

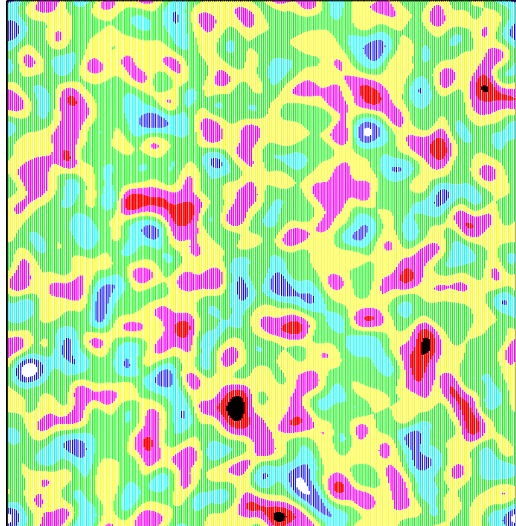
According to [15,20,21] one can write:

$$\Delta \tilde{T}^{k_d}(\vec{k}) = \sum_{j=1}^{N_{ps}} \gamma_j \sum_{\substack{|\vec{k}|=|\vec{k}_{max}| \\ |\vec{k}|=|\vec{k}_d|}} \cos(\vec{k}(\vec{x} - \vec{x}_j)) \quad (22)$$

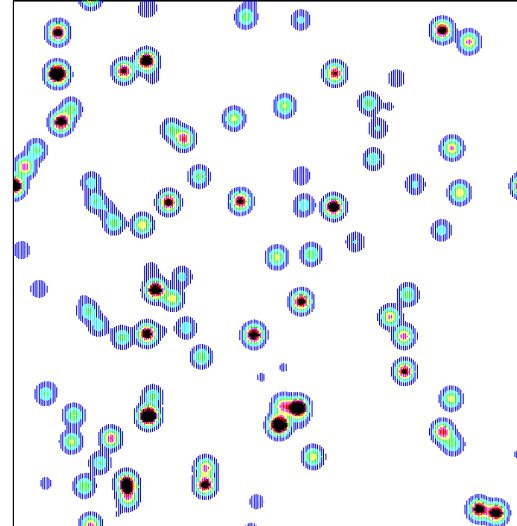
Therefore, the filtered function $\Delta \tilde{T}^{k_d}(\vec{k})$ at the point $\vec{x} = \vec{x}_j$ has a peak with amplitude equal to the power of j -th point source times the number of modes that we can use for data analysis in the appropriate experiment.

In our simulations of the signal+noise we use the standard CDM model and background of 100 point sources randomly distributed over the $10^\circ \times 10^\circ$ map. Without loss of generality we use the simple symmetric Gaussian antenna profile. All these calculations, of course, could be done for any arbitrary antenna beam. In Fig.8 we show the map of the CMB together with the maps of noise, CMB+noise and the filtered map of CMB+noise. The last one shows us more or less clearly the positions and powers of point sources. The significant anisotropy that appears in the last map occurs for the following reason. According to formulae [21] we use only the set of harmonics k_1, k_2 , that obey the relation $k_1^2 + k_2^2 > k_d^2$. Therefore, the number of horizontal and vertical waves is larger than the number of waves in any other direction. (This problem does not occur if we use spherical harmonics Y_l^m with $l > l_d$).

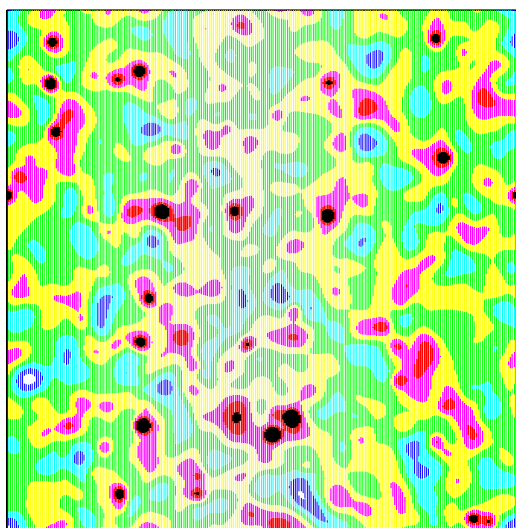
We apply the same iteration technique as in the previous section and therefore separate noise from the cosmological signal (Fig.9). It is necessary to note that each iteration removes an appropriate point source at the beginning of this process for the most powerful and separated sources. For the weaker sources, additional iterations are needed. The signal from the j -th source decreases as $\approx \frac{\gamma_j}{((\vec{k}_{max} - \vec{k}_d) \delta r)^2}$, where δr is the distance from the peak (in one dimension this dependence is linear).



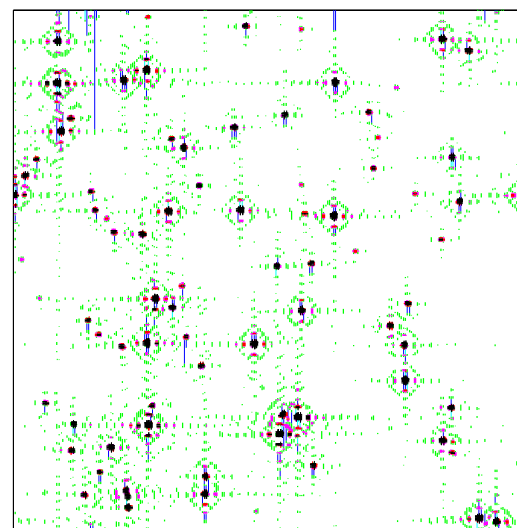
CMB



noise

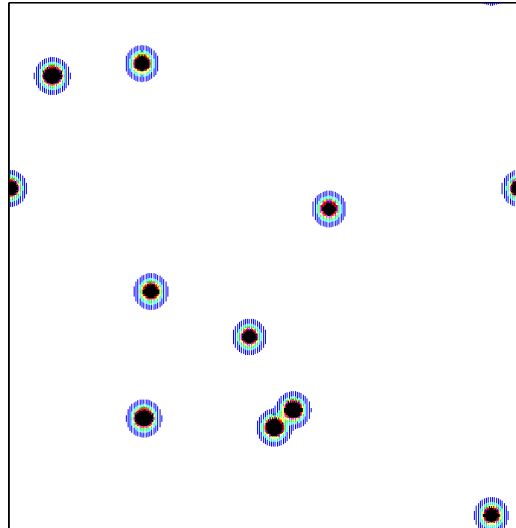


CMB + noise

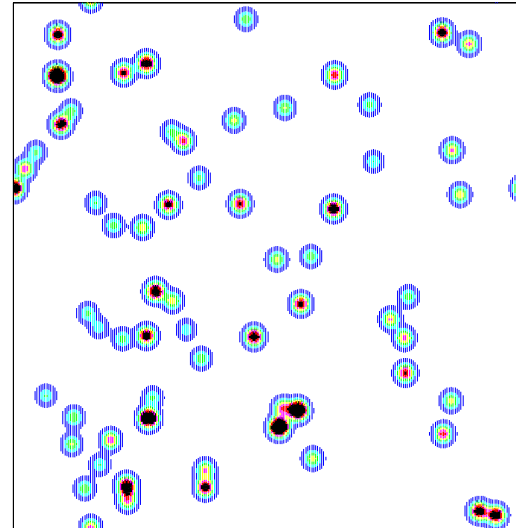


CMB + noise
after filtration

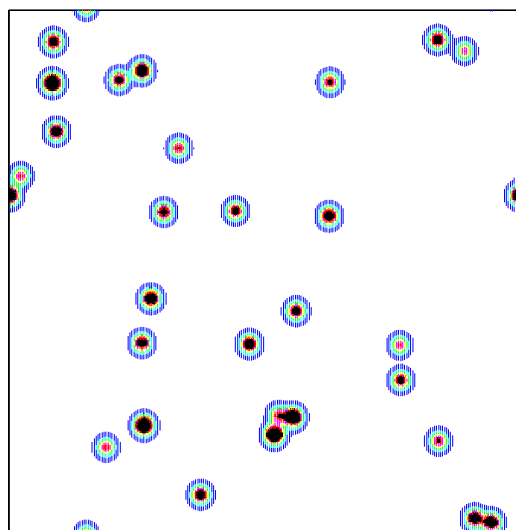
Fig. 8 Simulated sky maps of $10^\circ \times 10^\circ$.



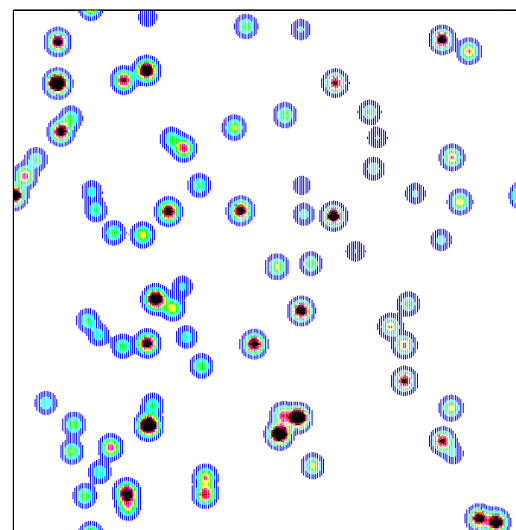
after 10 iterations



after 70 iterations



after 30 iterations



after 100 iterations

Fig. 9 Noise maps (i.e. removed sources) after different numbers of iterations. The size and shading of each source is proportional to its amplitude.

This affects the neighboring peaks and can change their amplitudes. Therefore, this approximation works if $((\vec{k}_{max} - \vec{k}_d)\delta r_{ij})^2 \ll \frac{\gamma_i}{\gamma_j}$, where r_{ij} is the separation between the i-th and j-th peaks (the i-th peak is the closest to the j-th peak). Otherwise, the amplitudes that have been found in each iteration would not correspond to the powers of the sources and we therefore have to perform a number of iterations that is larger than the number of sources.

4 Conclusions

In this paper we present a powerful method for extraction of unresolved point sources from future high resolution CMB maps (such as MAP, Planck, VSA, CBI, DASY, AMI and RATAN 600). Our method is based on the distribution of phases. The most important advantage of our technique is that we do not make any strong assumptions about the expected CMB signal as well as about the antenna profile. Most other techniques use the estimated power spectrum of the CMB and noise before the data analysis is implemented (e.g. Wiener filter) or they require special assumptions about the antenna profile (e.g., wavelets techniques). It is worth stressing that, for example, assumptions about the CMB power spectrum can lead to incorrect interpretations of the observational data. Roughly speaking, by making such assumptions, one runs the risk of generating the result one wants and any discrepancies are considered to be errors.

Our algorithm is numerically very efficient. It is a linear algorithm and requires $N \ln(N) \times N_{ps}$ operations, where N is the number of pixels. Therefore it can be easily applied to the analysis of large data sets. We have demonstrated the accuracy which can be achieved using our algorithm to remove the contribution from point sources on all scales. We believe that this technique is potentially a very powerful tool for extracting this type of noise from future high resolution maps.

Acknowledgments

We are very grateful to I.Novikov and A.Doroshkevich for discussions and P.Coles and R.Scherrer for informative communications. This investigation was partly supported by INTAS under grant number 97-1192, by RFFI under grant 17625 and by Danmarks Grundforskningfond through its support for TAC.

References

- Banday, A.J., Gorski, K.M., Bennett, C.L., Hinshaw, G., Kogut, A., & Smoot, G.F., ApJ. Letters, **468**, 85, 1996
- Bond, J.R., A.N.Jaffe and L.Knox, Phys. Rev. D. 57, 2117, 1998.
- Bouchet, F.R. & Gispert, R. 1999, astro-ph/9903176
- Cayon, L., Sanz, J.L., Barreiro., R.B., Martinez-Gonzalez, E., Vielva, P., Toffolatti, L., Silk, J., Diego, J.M. and F. Argueso astro-ph/9912471
- Coles, P. and L.Y.Chiang, MNRAS, **311**, 809, 2000a.
- Coles, P. and L.Y.Chiang, Nature, **406**, 376-378, 2000b.
- Hobson, M.P., Barreiro, R.B., Toffolatti, L., Lasenby, A.N., Sanz, J.L., Jones, A.W. &

Bouchet, F.R. 1999, MNRAS, 306, 232.

Gorski, K.M., Proceedings of the 31-st Recontres de Marion Astrophysics Meeting, p. 77, 1997, astro-ph/9701191.

Guiderdony, B. 1999, astro-ph/9903112

Melott, A., S. Shandarin and R. Scherrer, ApJ. **377**, 79, 1991.

Novikov, D.I., Naselsky, P.D., Jorgensen, H.E., Christensen, P.R., Novikov, I.D., Norgaarrd-Nielsen, H.U., astro-ph/0001432

Sanz, J.L., Barreiro, R.B., Cayon, L., Martinez-Gonzalez, E., Ruiz, G.A., Diaz, F.J., Argueso, F., Silk, J., and L. Toffolatti, 1999, astro-ph/9909497

Tegmark, M. & Efstathiou, G. 1996, MNRAS, 281, 1297.